Exosomes derived from umbilical cord mesenchymal stem cells repair blood-spinal cord barrier disruption after spinal cord injury through down-regulation of endothelin-1

Chenhui Xue [1], **Xun Ma** [Corresp., 1, 2], **Xiaoming Guan** [Corresp., 1, 2], **Haoyu Feng** [1, 2], **Mingkui Zheng** [1], **Xihua Yang** [3]

[1] Third Hospital of Shanxi Medical University, Shanxi Bethune Hospital, Shanxi Academy of Medical Sciences, Tongji Shanxi Hospital, Taiyuan, Shanxi, China

[2] Department of Orthopedics, Shanxi Bethune Hospital, Shanxi Academy of Medical Sciences, Tongji Shanxi Hospital, Third Hospital of Shanxi Medical University, Taiyuan, Shanxi, China

[3] Laboratory Animal Center, Shanxi Province Cancer Hospital/Shanxi Hospital Affiliated to Cancer Hospital, Chinese Academy of Medical Sciences/Cancer Hospital Affiliated to Shanxi Medical University, Taiyuan, Shanxi, China

Corresponding Authors: Xun Ma, Xiaoming Guan
Email address: maxun2532@sina.com, doctor_gxm2012@126.com

Spinal cord injury could cause irreversible neurological dysfunction by destroying the blood-spinal cord barrier (BSCB) and allowing blood cells like neutrophils and macrophages to infiltrate the spinal cord. Exosomes derived from mesenchymal stem cells (MSCs) found in the human umbilical cord have emerged as a potential therapeutic alternative to cell-based treatments. This study aimed to investigate the mechanism underlying the alterations in the BSCB permeability by human umbilical cord MSC-derived exosomes (hUC-MSCs-Exos) after SCI. First, we used hUC-MSCs-Exos to treat SCI rat models, s demonstrating their ability to inhibit BSCB permeability damage, improve neurological repair, and reduce SCI-induced upregulation of prepro-endothelin-1 (prepro-ET-1) mRNA and endothelin-1 (ET-1) peptide expression. Subsequently, we confirmed that hUC-MSCs-Exos could alleviate cell junction destruction and downregulate MMP-2 and MMP-9 expression after SCI, contributing to BSCB repair through ET-1 inhibition. Finally, we established an *in vitro* model of BSCB using human brain microvascular endothelial cells and verified that hUC-MSCs-Exos could increase theexpression ofjunction proteins in endothelial cells after oxygen-glucose deprivation by ET-1 downregulation. This study indicates that hUC-MSCs-Exos could help maintain BSCB's structural integrity and promote functional recovery by suppressing ET-1 expression.

Exosomes Derived from Umbilical Cord Mesenchymal Stem Cells Repair Blood-Spinal Cord Barrier Disruption after Spinal Cord Injury through Down-Regulation of Endothelin-1

Chenhui Xue[1], Xun Ma[1,2*], Xiaoming Guan[1,2*], Haoyu Feng[1,2], Mingkui Zheng[1], Xihua Yang[3]

[1] Third Hospital of Shanxi Medical University, Shanxi Bethune Hospital, Shanxi Academy of Medical Sciences, Tongji Shanxi Hospital, Taiyuan, 030032, China
[2] Department of Orthopedics, Shanxi Bethune Hospital, Shanxi Academy of Medical Sciences, Tongji Shanxi Hospital, Third Hospital of Shanxi Medical University, Taiyuan, 030032, China
[3] Laboratory Animal Center, Shanxi Province Cancer Hospital/Shanxi Hospital Affiliated to Cancer Hospital, Chinese Academy of Medical Sciences/Cancer Hospital Affiliated to Shanxi Medical University, 030013, Taiyuan, Shanxi, China

Corresponding Author:
Xun Ma[1,2]
[1] Third Hospital of Shanxi Medical University, Shanxi Bethune Hospital, Shanxi Academy of Medical Sciences, Tongji Shanxi Hospital, Taiyuan, 030032, China
[2] Department of Orthopedics, Shanxi Bethune Hospital, Shanxi Academy of Medical Sciences, Tongji Shanxi Hospital, Third Hospital of Shanxi Medical University, Taiyuan, 030032, China
Email address: maxun2532@sina.com

Corresponding Author:
Xiaoming Guan[1,2]
[1] Third Hospital of Shanxi Medical University, Shanxi Bethune Hospital, Shanxi Academy of Medical Sciences, Tongji Shanxi Hospital, Taiyuan, 030032, China
[2] Department of Orthopedics, Shanxi Bethune Hospital, Shanxi Academy of Medical Sciences, Tongji Shanxi Hospital, Third Hospital of Shanxi Medical University, Taiyuan, 030032, China
Email address: doctor_gxm2012@126.com

Abstract

Spinal cord injury could cause irreversible neurological dysfunction by destroying the blood-spinal cord barrier (BSCB) and allowing blood cells like neutrophils and macrophages to infiltrate the spinal cord. Exosomes derived from mesenchymal stem cells (MSCs) found in the

human umbilical cord have emerged as a potential therapeutic alternative to cell-based treatments. This study aimed to investigate the mechanism underlying the alterations in the BSCB permeability by human umbilical cord MSC-derived exosomes (hUC-MSCs-Exos) after SCI. First, we used hUC-MSCs-Exos to treat SCI rat models, s demonstrating their ability to inhibit BSCB permeability damage, improve neurological repair, and reduce SCI-induced upregulation of prepro-endothelin-1 (prepro-ET-1) mRNA and endothelin-1 (ET-1) peptide expression. Subsequently, we confirmed that hUC-MSCs-Exos could alleviate cell junction destruction and downregulate MMP-2 and MMP-9 expression after SCI, contributing to BSCB repair through ET-1 inhibition. Finally, we established an in vitro model of BSCB using human brain microvascular endothelial cells and verified that hUC-MSCs-Exos could increase the expression of junction proteins in endothelial cells after oxygen-glucose deprivation by ET-1 downregulation. This study indicates that hUC-MSCs-Exos could help maintain BSCB's structural integrity and promote functional recovery by suppressing ET-1 expression.

Introduction

Spinal cord injury (SCI), a central nervous system (CNS) disorder, is characterized by persistent sensory and motor abnormalities. Due to its high morbidity and death, SCI poses a global health burden(Simpson et al., 2012; Ahuja et al., 2017). Injury to neurons and axons directly causes the majority of primary spinal cord injuries, whereas "Spinal cord microenvironment imbalance" is thought to be the cause of secondary spinal cord injury exacerbation(Fan et al., 2018). Restoration of neurological function following SCI is dependent on the integrity of the blood-spinal cord barrier (BSCB), which consists of continuous endothelial cells joined by molecular junctions. The BSCB also serves as a barrier to prevent paracellular and transcellular movement(Jin et al., 2021). Additionally, it may control and limit the entry of outside chemicals into the CNS, maintain the microenvironment's homeostasis, and significantly influence the pathophysiological process of various neurological illnesses(Bartanusz et al., 2011).

Human umbilical cord mesenchymal stem cells (hUC-MSCs) have emerged as a promising source of human stem cells for therapeutic interventions due to their widespread availability and minimal ethical concerns(Ullah, Subbarao & Rho, 2015). Transplantation of hUC-MSCs into traumatic spinal cord injuries has shown neuro regenerative properties and improved functional outcomes(Gao et al., 2020). However, similar to other cell-based therapies, hUC-MSC transplantation carries potential risks, including infections, embolism, acute immunogenicity, chronic immunogenicity, and tumorigenicity(Saeedi, Halabian & Imani Fooladi, 2019).

Exosomes are small extracellular vesicles ranging from 30 to 100 nm produced by all cells(Zhang et al., 2019). They are essential components of paracrine secretions and mediate cell-to-cell communication by transferring genetic material signals, such as non-coding RNAs and mRNAs, as well as proteins, and inhibiting their degradation(Hessvik & Llorente, 2018). Stem cell-derived exosomes exhibit therapeutic benefits comparable to stem cell transplantation

through mechanisms such as anti-apoptosis, immunomodulation, anti-inflammatory effects, and the promotion of angiogenesis(Han et al., 2016).

Endothelin (ET) is a potent vasoconstrictor involved in various responses associated with CNS disorders(Leslie et al., 2004),(Hostenbach et al., 2016). Endothelin-1 (ET-1) levels have been found to increase in the cerebrum tissue of traumatic brain injury (TBI) models and spinal cord tissue of SCI models(Maier et al., 2007; A et al., 2019; Michinaga et al., 2020). Overexpression of ET-1 causes loss of endothelial integrity, increases blood-brain barrier permeability, aggravates ischemia and hypoxia, as well as induces tissue necrosis and apoptosis(Peters et al., 2003).

Currently, SCI presently has limited effective therapeutic options due to its refractory nature. Human umbilical cord mesenchymal stem cell exosomes (hUC-MSCs-Exos) offers a promising approach to SCI treatment(Kang & Guo, 2022). However, their effectiveness and underlying mechanisms remain incompletely understood. Therefore, in this study, we investigated the function of hUC-MSCs-Exos in BSCB repair after SCI, focusing on the involvement of ET-1.

Materials & Methods

Cell culture

The HUC-MSCs were purchased from Fuyuan Biotechnology (Fuyuan Biotechnology Co., Ltd. Shanghai, CHINA). Cells were cultured in Dulbecco's modified Eagle's medium (DMEM, Gibco, NY, USA) supplemented with 10% fetal bovine serum (FBS, Gibco, NY, USA) and 1% penicillin/streptomycin (Thermo Fisher Scientific, Waltham, MA, USA). Human brain microvascular endothelial cells (HBMECs) were purchased from Meisen Cell Technology (Meisen Cell Technology, Zhejiang, China). Cells were cultured in an endothelial cell medium (ScienCell Research Laboratories, San Diego, CA, USA) and incubated in a humidified atmosphere at 5% CO2 and 37 °C.

Exosome isolation and characterization

To isolate exosomes, the hUMSC-conditioned medium was first centrifuged at 500 g for 10 minutes to remove cells. Subsequently, the supernatant was centrifuged at 10,000 g for 30 minutes to eliminate apoptotic vesicles and other debris. The resulting liquid was then filtered through a 0.22 mm filter. The exosomes were then collected as a pellet using ultracentrifugation (Beckman Optima XPN, 45Ti) at 110,000 g for 70 minutes. The exosome pellet was resuspended in phosphate-buffered saline (PBS) for purification and subjected to another round of ultracentrifugation at 110,000 g for 70 minutes to remove the contaminating proteins. Finally, the exosomes were resuspended in PBS and stored at -80 °C until further use. The Pierce BCA Protein Assay Kit (Thermo Fisher Scientific, Waltham, MA, USA) was used to assess the protein

content of the exosomes. The size of exosomes was determined by nanoparticle tracking analysis (NTA) using ZetaView S/N 17-310 (Particle Metrix, Meerbusch, Germany) along with its associated software. Additionally, transmission electron microscopy (TEM; JEOL Ltd., Tokyo, Japan) was used to morphologically examine isolated exosomes. Western blot analysis was utilized to determine the levels of CD63 (Abcam, Cambridge, UK) and TSG101 (Abcam, Cambridge, UK) in exosomes.

Experimental animals

All animal experimental protocols conformed to the Guide for the Care and Use of Laboratory Animals from the National Institutes of Health (NIH Publications No. 8023), and all procedures were approved by the Shanxi Provincial People's Hospital Institutional Animal Care and Use Committee (Approval No. 2022-089). Adult female Sprague–Dawley rats weighing between 220 and 250 g were obtained from the Laboratory Animal Center of Shanxi Cancer Institute (animal production certificate # SCXK (Jin) 2017-0001; Shanxi, China). The entire experimental process was conducted at the same institution (animal usage certificate # SYXK (Jin) 2017-0003; Shanxi, China). Rats were housed in pathogen-free environments, with two to three animals per cage. They were provided with a standard commercial diet, had ad libitum access to water, and maintained under control humidity (40-60%) in a 12-hour light-dark cycle. After the assay, all the surviving animals were euthanized by an intraperitoneal injection of barbiturates at the Laboratory Animal Center of Shanxi Cancer Institute. The rats were randomly assigned to the following four groups: control (n = 20), SCI (n = 20), exo (n = 20), and ET-1 (n = 20) groups.

Spinal cord injury and treatment

Rats were anesthetized with 1% sodium pentobarbital (3 mL/kg, i.p.), and a median dorsal incision was performed at the T10 segment. The surrounding tissues were carefully dissected to expose the T10 vertebral body, spinous process, and spinal cord. The muscles were dissected layer by layer while preserving the integrity of the dura mater. In the sham-operated group, the wound was sutured layer by layer after sterilization. A spinal cord injury model was established using the modified Allen's method for the remaining three groups. The spinal cord injury was created at the T10 level using a standardized force (10 g×5 cm), and the successful modeling was confirmed by the presence of congestion, edema, double hind limb convulsions, and spastic tail swing at the site of injury in the spinal cord.

Treatment

Postoperatively, the ET-1 group was injected 10 μL (1 μg/mL) of ET-1 directly into the injured site using a microinjector. The wound was subsequently sutured layer by layer after rinsing with saline and disinfection. The Sham and SCI groups were administered 200 μL PBS solution in the tail vein immediately after injury and 1 and 2 days post-injury, while 200 μL exosome (200 μg/mL) solution was administered to the Exos and ET-1 groups. All rats were given

intraperitoneal penicillin (200,000 U/d) for 3 days, while their bladder was manually massaged twice or thrice daily to facilitate urination until the urinary function was restored.

Behavioral tests

The Basso, Beattie, and Bresnahan (BBB) ratings were used to assess the functional impairments following SCI. Two independent examiners blinded to the experimental groups evaluated the BBB scores on an open-field scale. Evaluations were performed at 1, 3, 5, 7, 14, and 21 days after surgery to monitor the progression of functional recovery in the rats.

Western blot analysis

For western blot analysis, spinal cord tissue was mixed with RIPA lysate, lysed on ice for 30 min, and then centrifuged at 15 000×g for 10 min at 4° C. For protein analysis in vitro, HBMECs were lysed in RIPA buffer with protease and phosphatase inhibitors. The protein content of the supernatants was quantified using the PierceTM BCA protein assay kit (Thermo Fisher Scientific, Waltham, MA, USA), and the supernatant was collected for subsequent protein analysis. A 10% gel was used to separate equivalent quantities of 20 mg of protein, which were then transferred onto a polyvinylidene difluoride (PVDF) membrane (Merck Millipore, Darmstadt, Germany). Following blocking with 5% nonfat milk in TBS with 0.05% Tween 20 for 1 hour, the membrane was incubated with primary antibodies against ZO-1 (61-7300; Thermo Fisher Scientific), beta-catenin (ab32572, Abcam, Cambridge, UK), occluding (ab216327, Abcam), claudin-5 (352500; Santa Cruz Biotechnology, Inc., Dallas, TX, USA), MMP-2 (ab92536, Abcam), and MMP-9 (ab76003, Abcam) at 4°C overnight (around 20 hours). After three TBS-T washes, the membranes were incubated with the secondary antibodies for 1 hour at room temperature. The protein bands were visualized using an automated gel imaging system (Bio-Rad ChemiDoc MP, Bio-Rad, Hercules, CA, USA), while the band densities were measured using ImageJ software. The relative density ratios normalized to the Sham or Control group were used to describe the findings.

Real-Time PCR

Spinal cord tissue samples were subjected to isopropanol precipitations after total RNA extraction using the RNAiso plus protocol (TaKaRa Bio Inc., Shiga, Japan). The extracted total RNA was used to synthesize first-strand cDNA. Quantitative reverse transcription-polymerase chain reaction (RT-PCR) was used to measure mRNA levels using SYBR Green fluorescent probes. The SYBR Green Master Mix (TaKaRa Bio Inc., Shiga, Japan) was added to each reverse-transcription product, and the reaction mixture was then subjected to amplification using a CFX96 Touch Real-Time PCR Detection System (Bio-Rad, Hercules, CA, USA).
The following primer pairs were used for amplification:
Prepro-ET-1 Forward: 5′ -GTGAGAACGGCGGGGAGAAAC-3′

Reverse: 5′ - AATGATGTCCAGGTGGCAGAAGTAG -3′

GAPDH: Forward: 5′ -CTCTGATTTGGTCGTATTGGG-3′

Reverse: 5′ -TGGAAGATGGTGATGGGA TT-3′

Serial dilutions of each amplicon were also amplified to generate standard curves for the quantification of the PCR products. The copy numbers of each PCR product, equal to 1 μg of total RNA, was used to calculate the quantity of mRNA. The prepro-ET-1 mRNA expression levels were normalized to GAPDH values.

Evans Blue Dye Assays

Evans Blue Dye Assays were performed to assess BSCB permeability. A 2% Evans blue saline solution (2 mL/kg) was administered into the tail vein of rats 7 days after SCI. After 2 hours, the rats were anesthetized with 1% sodium pentobarbital (3 mL/kg), and saline was perfused through the heart until clear fluid began to flow from the right atrium. A 1 cm segment of the injured spinal cord, centered around the injury site, was carefully dissected, weighed, and homogenized in a 50% trichloroacetic acid solution. The homogenate was then centrifuged at 10,000 g for 10 min, and the supernatant was collected. The absorbance of the sample was measured using a spectrophotometer (with an excitation wavelength of 620 nm and an emission wavelength of 680 nm). The established standard curve was used to determine the quantity of Evans dye present in the tissue (μg/g).

FITC-Dextran Assays

The rats received an intravenous injection of 2% FITC-dextran (MW 70 kDa, 4 mg/kg; Sigma-Aldrich) solution in PBS via the tail vein 1 day after SCI. After 2 hours, the rats were injected with 10% chloral hydrate, followed by perfusion with 0.9% normal saline. The FITC-dextran-damaged spinal cord tissues were weighed, homogenized in PBS, and centrifuged. The optical density of the supernatant was measured using a spectrophotometer at an excitation wavelength of 493 nm and an emission wavelength of 517 nm to assess the presence of FITC-dextran.

Oxygen–glucose deprivation/reoxygenation procedure

Oxygen–glucose deprivation/reoxygenation (OGD/R) procedures were conducted following previously established protocols(Sun et al., 2017). Briefly, cultivated HBMECs were washed thrice with PBS and then transferred to serum-free DMEM without glucose (Gibco, Life Technologies, USA). Subsequently, the HBMECs were subjected to oxygen-glucose deprivation (OGD) by placing them in an anaerobic chamber containing 1% O2, 5% CO2, and 94% N2 at 37°C for 6 hours. After being exposed to OGD for 6 hours, the HBMECs were washed once with PBS and then incubated under normal conditions (reoxygenation) for 24 hours.

Cell viability assay

Cell counting kit-8 (CCK-8) assay was used to assess cell viability. HBMECs were cultured in endothelial cell media and seeded in 96-well plates. After 1, 2, 3, 4, and 5 days of incubation, 10 μl of CCK-8 reagent (Dojindo, Japan) was added to the culture medium. A microplate reader (Bio-Rad 680, Hercules, USA) was then used to measure the absorbance of each well at 450 nm.

Paracellular permeability assay

HBMECs were seeded overnight in a 200-μl medium at a density of 1 × 105 cells/well on Transwell permeable supports (PET membrane 24-well cell culture inserts with 0.4-μm pore size; Corelle; Corning Life Sciences, Corning, NY, USA). Subsequently, the cells were subjected to OGD for 6 hours, followed by reoxygenation for 22 hours (OGD6h/R22h). The cells were then exposed to media containing FITC-dextran (1 mg/ml) for 2 hours. The amount of FITC-dextran passing through the Transwell (in the lower chambers) was determined using an enzyme-labeled meter with an excitation wavelength of 493 nm and an emission wavelength of 517 nm.

Statistical analysis

All the experiments were performed three times at least. All data are shown as mean ± standard deviation, and statistical analysis was performed in GraphPad Prism (version 8.0, GraphPad Software Inc., USA). One-way ANOVA followed by Tukey's post hoc analysis was used for multiple comparisons. P-value < 0.05 was considered statistically significant.

Results

HUC-MSCs-Exos attenuate SCI-induced BSCB disruption

The successful isolation of the hUC-MSCs-Exos was confirmed by TEM, which revealed their characteristic cup-shaped morphology (Fig. 1A). The hUC-MSCs-Exos isolates were further identified using NTA, showing that particles with a diameter of 100 to 140 nm were the predominant populations (Fig. 1B). Western blot analysis of the exosome lysates demonstrated significant positive bands for CD63 and TSG101, indicating the presence of exosomal markers, while GAPDH was employed as a control for purity (Fig. 1C).
The BBB scores were utilized to evaluate the functional recovery. Comparison of locomotor activity between the Exo group and the SCI Group 3–21 days post-injury revealed a remarkable improvement in locomotor function following exosome therapy (Fig. 1D). Evaluation of BSCB integrity was performed using Evans blue and FITC-dextran fluorescence assays. HUC-MSCs-Exos significantly reduced the fluorescence intensity of Evans blue in the injured spinal cord (Fig. 1E), and the penetration of FITC-dextran (Fig. 1F). Collectively, these findings demonstrate that hUC-MSCs-Exos mitigate BSCB disruption in rats after SCI.

HUC-MSCs-Exos increase SCI-induced ET-1 production

Previous studies demonstrated an increase in ET-1 levels in the spinal cord tissue of SCI rats, suggesting that excessive ET-1 production following SCI contributes to vasoconstriction, which is closely associated with spinal cord ischemia and hypoxia symptoms(A et al., 2019). Therefore, we examined the effects of hUC-MSCs-Exos on SCI-induced ET-1 production. Our results revealed a significant increase in the expression of prepro-ET-1 mRNA and ET-1 peptide following SCI. However, the administration of hUC-MSCs-Exos at 200 ug/day after SCI reduced the SCI-induced upregulation of prepro-ET-1 mRNA (Fig. 2A) and ET-1 peptide (Fig. 2B).

ET-1 is involved in the effects of hUC-MSCs-Exos on SCI repair

To investigate the role of ET-1 in the cell neurological repair effects of hUC-MSCs-Exos on the BSCB after SCI, ET-1 was administered at the injury site after SCI. Our results demonstrated that ET-1 injection significantly reduced the therapeutic effect of exosomes on motor activity 3-21 days post-SCI (Figure 3A). Furthermore, at 24 hours following SCI, Evans blue dye extravasation was assessed. The findings of the Evans blue dye (Fig. 3B) and Evans blue extravasation tests (Fig. 3C) revealed that ET-1 reversed the protective effect conferred by hUC-MSCs-Exos. Additionally, FITC-dextran penetration, which was decreased by the administration of hUC-MSCs-Exos, was significantly increased following ET-1 injection (Fig. 3D). According to the aforementioned data, hUC-MSCs-Exos enhances functional recovery and lessens BSCB disruption following SCI via ET-1.

HUC-MSCs-Exos increase the expression of junction proteins after SCI by downregulation of ET-1

We performed a Western blot analysis to examine whether hUC-MSCs-Exos can protect the integrity of the BSCB by regulating tight junction proteins and adhesion junction proteins. Our results demonstrated a significant reduction in the expression levels of ZO-1, β-catenin, occludin, and claudin-5 following SCI. However, treatment with hUC-MSCs-Exos attenuated these changes, thereby promoting the restoration of BSCB integrity. Notably, the therapeutic effect of exosomes was also significantly compromised upon ET-1 injection (Fig. 4A-4E). According to the aforementioned data, hUC-MSCs-Exos enhances expression of cell junction proteins following SCI via downregulation of ET-1.

HUC-MSCs-Exos decreases expression of inflammatory mediators in SCI rats by downregulation of ET-1

Previous studies have highlighted the crucial role of matrix metalloproteinase (MMP) in the recovery process following SCI(Yu et al., 2008). Notably, MMP-2 and MMP-9 are known to be modulated by ET-1(He, Prasanna & Yorio, 2007; Wang et al., 2010). Therefore, we subsequently evaluated the levels of MMP-2 and MMP-9 to confirm that the impact of hUC-MSCs-Exos therapy in SCI rats was caused by the reduced expression of ET-1. Western blot

analysis revealed significantly elevated expression levels of MMP-2 and MMP-9 in SCI rats compared to the Sham group. However, the administration of HUC-MSCs-Exos resulted in a significant decrease in MMP-2 and MMP-9 expression. The therapeutic effect of exosomes was reduced upon ET-1 injection (Fig. 5A-5C).

HUC-MSCs-Exos increase the expression of junction proteins in HBMECs after OGD/R by downregulation of ET-1

To detect the effects of hUC-MSCs-Exos on OGD/R-injured HBMECs, we conducted a series of experiments, including Western blot analysis, Cell Viability Assay, and Paracellular Permeability Assay. The expressions of junctional proteins, including Claudin-5, Occludin, beta-Catenin, and ZO-1, were significantly decreased in HCMECs subjected to OGD/R. However, the presence of hUC-MSCs-Exos notably reversed this decrease in expression, and this therapeutic effect was reduced upon ET-1 administration (Fig. 5A-E). Moreover, we detected that hUC-MSCs-Exos significantly enhanced cell viability, whereas ET-1 exerted an inhibitory effect (Fig. 5F). To investigate the impact of OGD/R and ET-1 on the integrity of HBMECs, FITC-dextran was added to the cells. Our results confirmed that OGD/R significantly increased cell permeability, while hUC-MSCs-Exos addition significantly attenuated this effect. Interestingly, the introduction of ET-1 significantly increased endothelial barrier permeability (Fig. 5G).

Discussion

In this study, we demonstrated that hUC-MSCs-Exos mitigate neurological impairments by preserving the integrity of the BSCB in SCI-affected rats. We demonstrated that hUC-MSCs-Exos suppress ET-1 expression, thereby preventing the disruption of cell junctions following SCI, facilitating BSCB repair. Our study sheds light on the underlying mechanism through which hUC-MSCs-Exos exert their influence on BSCB integrity after SCI.

Growing evidence indicates that the BSCB may be indispensable to the pathophysiology of SCI(Jin et al., 2021). This barrier maintains the homeostasis of the spinal cord by regulating molecular exchanges between blood vessels and spinal parenchyma(Abbott et al., 2010). However, in clinical settings and animal models, SCI often leads to BSCB destruction, resulting in morphological and functional changes, such as vascular alterations, increased permeability, spinal cord edema, and spinal cord cavity formation(Jin et al., 2021)[,5]. Mesenchymal stem cells derived exosomes have been shown to impact various processes, such as neuronal apoptosis, angiogenesis, and inflammation in SCI.(Liu et al., 2019) However, their role in BSCB repair remains an ongoing investigation. In our current study, we performed various assays for BSCB permeability, such as Evans Blue Dye Assays, FITC-Dextran Assays, and Paracellular Permeability Assay, in SCI-model rats, with or without exosome treatment. Our findings demonstrate that hUC-MSCs-Exos effectively reduce neurological impairments by preserving the integrity of the BSCB in rats with SCI.

Tight junctions between individual endothelial cells highly regulate the paracellular diffusion pathway in brain capillary endothelial cells(Abbott et al., 2010). Among the plasma membrane proteins responsible for the formation of tight junctions are claudin, occludin, and adherens junction molecules. The zonula occludens protein and cingulin form the cytoplasmic components of tight junctions(Abbott, Rönnbäck & Hansson, 2006; Bernacki et al., 2008). We examined tight junction membrane proteins and cytoplasmic components, such as claudin-5, Occluding, β-Catenin, and ZO-1, using Western blot analysis. Our results confirmed that hUC-MSCs-Exos regulate the expression of tight junction proteins, thereby alleviating BSCB disruption after SCI.

Matrix metalloproteinases (MMPs) are a family of zinc-containing peptidases secreted by neutrophils. These peptidases destroy and restructure the extracellular matrix as well as other extracellular proteins. Matrix metalloproteinases are an essential component of barrier function(Beck et al., 2010). MMPs could instantly infiltrate the parenchyma of the spinal cord following the injury and continue to reside at the lesion site for more than 10 days(Carlson et al., 1998). MMPs, particularly MMP-2 and MMP-9, are prominently expressed 7 days after SCI and contribute to BSCB breakdown under pathological conditions(Yao et al., 2018; Wang et al., 2021). Our study also revealed elevated expression of MMP-2 and MMP-9 in the spinal cord tissue of rats after SCI. Administration of hUC-MSCs-Exos decreased the expression of MMP-2 and MMP-9, indicating that hUC-MSCs-Exos could mitigate BSCB disruption mediated by these MMPs. Our findings also provide further insight into the molecular mechanisms underlying the protective effects of exosomes on BSCB disruption after SCI.

Notably, our results show that the beneficial effects of hUC-MSCs-Exos on SCI were significantly inhibited in the presence of ET-1, a vasoconstrictive peptide composed of 21 amino acids. Increased expression of ET-1 has been correlated with the pattern of BSCB degradation after SCI. Pharmacological blockade of ET-1–mediated vasoconstriction has been shown to attenuate BSCB degradation after SCI.(McKenzie et al., 1995) And intrathecal administration of ET-1 in the intact spinal cord resulted in disruption of the BSCB.(Westmark et al., 1995) In this study, ET-1 injection in the wound site significantly reduced the therapeutic effects of hUC-MSCs-Exos. *In vitro* experiments further demonstrated that hUC-MSCs-Exos increased the expression of tight junction and adhesion junction proteins, enhanced cell viability, and decreased cell permeability following OGD/R. Furthermore, the administration of ET-1 to HBMECs led to corresponding changes in the expression of tight junction proteins, adhesion junction proteins, cell viability, and permeability. These findings confirm that the regulatory effect of hUC-MSCs-Exos on BSCB function is mediated through the modulation of ET-1 expression.

It should be noted that there are some limitations to this study. First, exosomes consist of a class of nanovesicles that contain various substances derived from parental cells, such as miRNA, mRNA, and protein, and transport them to recipient cells (Kalluri and LeBleu, 2020). Exactly

which of these components exerted a role in regulating ET-1 and ameliorating BSCB destruction was not investigated in this study. These functional components need to be further identified in subsequent studies. Second, the spinal cord has a variety of cell types, each of which performs a distinctive function and interacts with others in the destruction of the BSCB after SCI. Due of this, microglia and astrocytes both contribute significantly to the development of BSCB destruction following SCI. In the current investigation, we only looked at how exosomes affected endothelial cells. It is important to carry out additional in vitro and in vivo research using co-culture systems with mixed endothelial cells and other spinal cord cell types. Third, the current study did not examine ET-1 receptors ETaR and ETbR or additional signalling pathways that are involved in ET-1 intracellular signalling. Future research will need to focus on these receptors and signalling pathways.

Conclusions

In conclusion, the current study provides evidence for the protective effect of hUC-MSCs-Exos on BSCB integrity following SCI. We demonstrate that hUC-MSCs-Exos attenuate BSCB degradation and promote functional recovery after SCI by regulating the expression of ET-1. We further elucidate the mechanism by which hUC-MSCs-Exos exert their influence on BSCB integrity after SCI.

Acknowledgements

We would like to thank the Shanxi Provincial Key Laboratory of Kidney Disease, the Core Laboratory at Shanxi Provincial People's Hospital and the Laboratory Animal Center at Shanxi Province Cancer Hospital for their technical support.
We thank Bullet Edits Limited for the linguistic editing and proofreading of the manuscript.

References

A J-C, Li Z-Y, Long Q-F, Wang D-Y, Zhao H-S, Jia S-L, Zhang W-H. 2019. MiR-379-5p improved locomotor function recovery after spinal cord injury in rats by reducing endothelin 1 and inhibiting astrocytes expression. *European Review for Medical and Pharmacological Sciences* 23:9738–9745. DOI: 10.26355/eurrev_201911_19536.

403 Abbott NJ, Patabendige AAK, Dolman DEM, Yusof SR, Begley DJ. 2010. Structure and
404 function of the blood-brain barrier. *Neurobiology of Disease* 37:13–25. DOI:
405 10.1016/j.nbd.2009.07.030.
406 Abbott NJ, Rönnbäck L, Hansson E. 2006. Astrocyte-endothelial interactions at the blood-brain
407 barrier. *Nature Reviews. Neuroscience* 7:41–53. DOI: 10.1038/nrn1824.
408 Ahuja CS, Wilson JR, Nori S, Kotter MRN, Druschel C, Curt A, Fehlings MG. 2017. Traumatic
409 spinal cord injury. *Nature Reviews. Disease Primers* 3:17018. DOI:
410 10.1038/nrdp.2017.18.
411 Bartanusz V, Jezova D, Alajajian B, Digicaylioglu M. 2011. The blood-spinal cord barrier:
412 morphology and clinical implications. *Annals of Neurology* 70:194–206. DOI:
413 10.1002/ana.22421.
414 Beck KD, Nguyen HX, Galvan MD, Salazar DL, Woodruff TM, Anderson AJ. 2010.
415 Quantitative analysis of cellular inflammation after traumatic spinal cord injury: evidence
416 for a multiphasic inflammatory response in the acute to chronic environment. *Brain: A*
417 *Journal of Neurology* 133:433–447. DOI: 10.1093/brain/awp322.
418 Bernacki J, Dobrowolska A, Nierwińska K, Małecki A. 2008. Physiology and pharmacological
419 role of the blood-brain barrier. *Pharmacological reports: PR* 60:600–622.
420 Carlson SL, Parrish ME, Springer JE, Doty K, Dossett L. 1998. Acute inflammatory response in
421 spinal cord following impact injury. *Experimental Neurology* 151:77–88. DOI:
422 10.1006/exnr.1998.6785.
423 Fan B, Wei Z, Yao X, Shi G, Cheng X, Zhou X, Zhou H, Ning G, Kong X, Feng S. 2018.
424 Microenvironment Imbalance of Spinal Cord Injury. *Cell Transplantation* 27:853–866.
425 DOI: 10.1177/0963689718755778.

426 Gao L, Peng Y, Xu W, He P, Li T, Lu X, Chen G. 2020. Progress in Stem Cell Therapy for
427 Spinal Cord Injury. *Stem Cells International* 2020:2853650. DOI:
428 10.1155/2020/2853650.
429 Han C, Sun X, Liu L, Jiang H, Shen Y, Xu X, Li J, Zhang G, Huang J, Lin Z, Xiong N, Wang T.
430 2016. Exosomes and Their Therapeutic Potentials of Stem Cells. *Stem Cells International*
431 2016:7653489. DOI: 10.1155/2016/7653489.
432 He S, Prasanna G, Yorio T. 2007. Endothelin-1-mediated signaling in the expression of matrix
433 metalloproteinases and tissue inhibitors of metalloproteinases in astrocytes. *Investigative*
434 *Ophthalmology & Visual Science* 48:3737–3745. DOI: 10.1167/iovs.06-1138.
435 Hessvik NP, Llorente A. 2018. Current knowledge on exosome biogenesis and release. *Cellular*
436 *and molecular life sciences: CMLS* 75:193–208. DOI: 10.1007/s00018-017-2595-9.
437 Hostenbach S, D'haeseleer M, Kooijman R, De Keyser J. 2016. The pathophysiological role of
438 astrocytic endothelin-1. *Progress in Neurobiology* 144:88–102. DOI:
439 10.1016/j.pneurobio.2016.04.009.
440 Jin L-Y, Li J, Wang K-F, Xia W-W, Zhu Z-Q, Wang C-R, Li X-F, Liu H-Y. 2021. Blood-Spinal
441 Cord Barrier in Spinal Cord Injury: A Review. *Journal of Neurotrauma* 38:1203–1224.
442 DOI: 10.1089/neu.2020.7413.
443 Kang J, Guo Y. 2022. Human Umbilical Cord Mesenchymal Stem Cells Derived Exosomes
444 Promote Neurological Function Recovery in a Rat Spinal Cord Injury Model.
445 *Neurochemical Research* 47:1532–1540. DOI: 10.1007/s11064-022-03545-9.
446 Leslie SJ, Rahman MQ, Denvir MA, Newby DE, Webb DJ. 2004. Endothelins and their
447 inhibition in the human skin microcirculation: ET[1-31], a new vasoconstrictor peptide.

British Journal of Clinical Pharmacology 57:720–725. DOI: 10.1111/j.1365-2125.2004.02074.x.

Liu W, Wang Y, Gong F, Rong Y, Luo Y, Tang P, Zhou Z, Zhou Z, Xu T, Jiang T, Yang S, Yin G, Chen J, Fan J, Cai W. 2019. Exosomes Derived from Bone Mesenchymal Stem Cells Repair Traumatic Spinal Cord Injury by Suppressing the Activation of A1 Neurotoxic Reactive Astrocytes. *Journal of Neurotrauma* 36:469–484. DOI: 10.1089/neu.2018.5835.

Maier B, Lehnert M, Laurer HL, Marzi I. 2007. Biphasic elevation in cerebrospinal fluid and plasma concentrations of endothelin 1 after traumatic brain injury in human patients. *Shock (Augusta, Ga.)* 27:610–614. DOI: 10.1097/shk.0b013e31802f9eaf.

McKenzie AL, Hall JJ, Aihara N, Fukuda K, Noble LJ. 1995. Immunolocalization of endothelin in the traumatized spinal cord: relationship to blood-spinal cord barrier breakdown. *Journal of Neurotrauma* 12:257–268. DOI: 10.1089/neu.1995.12.257.

Michinaga S, Inoue A, Yamamoto H, Ryu R, Inoue A, Mizuguchi H, Koyama Y. 2020. Endothelin receptor antagonists alleviate blood-brain barrier disruption and cerebral edema in a mouse model of traumatic brain injury: A comparison between bosentan and ambrisentan. *Neuropharmacology* 175:108182. DOI: 10.1016/j.neuropharm.2020.108182.

Peters CM, Rogers SD, Pomonis JD, Egnaczyk GF, Keyser CP, Schmidt JA, Ghilardi JR, Maggio JE, Mantyh PW. 2003. Endothelin receptor expression in the normal and injured spinal cord: potential involvement in injury-induced ischemia and gliosis. *Experimental Neurology* 180:1–13. DOI: 10.1016/s0014-4886(02)00023-7.

469 Saeedi P, Halabian R, Imani Fooladi AA. 2019. A revealing review of mesenchymal stem cells
470 therapy, clinical perspectives and Modification strategies. *Stem Cell Investigation* 6:34.
471 DOI: 10.21037/sci.2019.08.11.
472 Simpson LA, Eng JJ, Hsieh JTC, Wolfe DL, Spinal Cord Injury Rehabilitation Evidence Scire
473 Research Team. 2012. The health and life priorities of individuals with spinal cord injury:
474 a systematic review. *Journal of Neurotrauma* 29:1548–1555. DOI:
475 10.1089/neu.2011.2226.
476 Sun L, Li M, Ma X, Feng H, Song J, Lv C, He Y. 2017. Inhibition of HMGB1 reduces rat spinal
477 cord astrocytic swelling and AQP4 expression after oxygen-glucose deprivation and
478 reoxygenation via TLR4 and NF-κB signaling in an IL-6-dependent manner. *Journal of*
479 *Neuroinflammation* 14:231. DOI: 10.1186/s12974-017-1008-1.
480 Ullah I, Subbarao RB, Rho GJ. 2015. Human mesenchymal stem cells - current trends and future
481 prospective. *Bioscience Reports* 35:e00191. DOI: 10.1042/BSR20150025.
482 Wang H-H, Hsieh H-L, Wu C-Y, Yang C-M. 2010. Endothelin-1 enhances cell migration via
483 matrix metalloproteinase-9 up-regulation in brain astrocytes. *Journal of Neurochemistry*
484 113:1133–1149. DOI: 10.1111/j.1471-4159.2010.06680.x.
485 Wang X, Shi Q, Ding J, Liang J, Lin F, Cai B, Chen Y, Zhang G, Xu J, Lian X. 2021. Human
486 Bone Marrow Mesenchymal Stem Cell-Derived Exosomes Attenuate Blood-Spinal Cord
487 Barrier Disruption via the TIMP2/MMP Pathway After Acute Spinal Cord Injury.
488 *Molecular Neurobiology* 58:6490–6504. DOI: 10.1007/s12035-021-02565-w.
489 Westmark R, Noble LJ, Fukuda K, Aihara N, McKenzie AL. 1995. Intrathecal administration of
490 endothelin-1 in the rat: impact on spinal cord blood flow and the blood-spinal cord
491 barrier. *Neuroscience Letters* 192:173–176. DOI: 10.1016/0304-3940(95)11638-d.

492 Yao Y, Xu J, Yu T, Chen Z, Xiao Z, Wang J, Hu Y, Wu Y, Zhu D. 2018. Flufenamic acid
493 inhibits secondary hemorrhage and BSCB disruption after spinal cord injury.
494 *Theranostics* 8:4181–4198. DOI: 10.7150/thno.25707.
495 Yu F, Kamada H, Niizuma K, Endo H, Chan PH. 2008. Induction of mmp-9 expression and
496 endothelial injury by oxidative stress after spinal cord injury. *Journal of Neurotrauma*
497 25:184–195. DOI: 10.1089/neu.2007.0438.
498 Zhang Y, Liu Y, Liu H, Tang WH. 2019. Exosomes: biogenesis, biologic function and clinical
499 potential. *Cell & Bioscience* 9:19. DOI: 10.1186/s13578-019-0282-2.
500

Figure 1

HUC-MSCs-Exos attenuate SCI-induced BSCB disruption.

(A) TEM photomicrographs of hUC-MSCs -Exos; scale bar = 200nm. (B) NTA results of BMSC-Exos. (C) Western blotting showed the presence of exosomal markers, including CD63, and TSG101, in BMSC-Exos. (D) The BBB scores. *P < 0.05 versus the Sham group; **P < 0.01 versus sham-operated group; n = 3. (E) Quantification of the amount of Evans Blue at 7day (μg/g). (F) FITC-dextran was used in the spinal cord peripheral penetration analysis results at 7day.

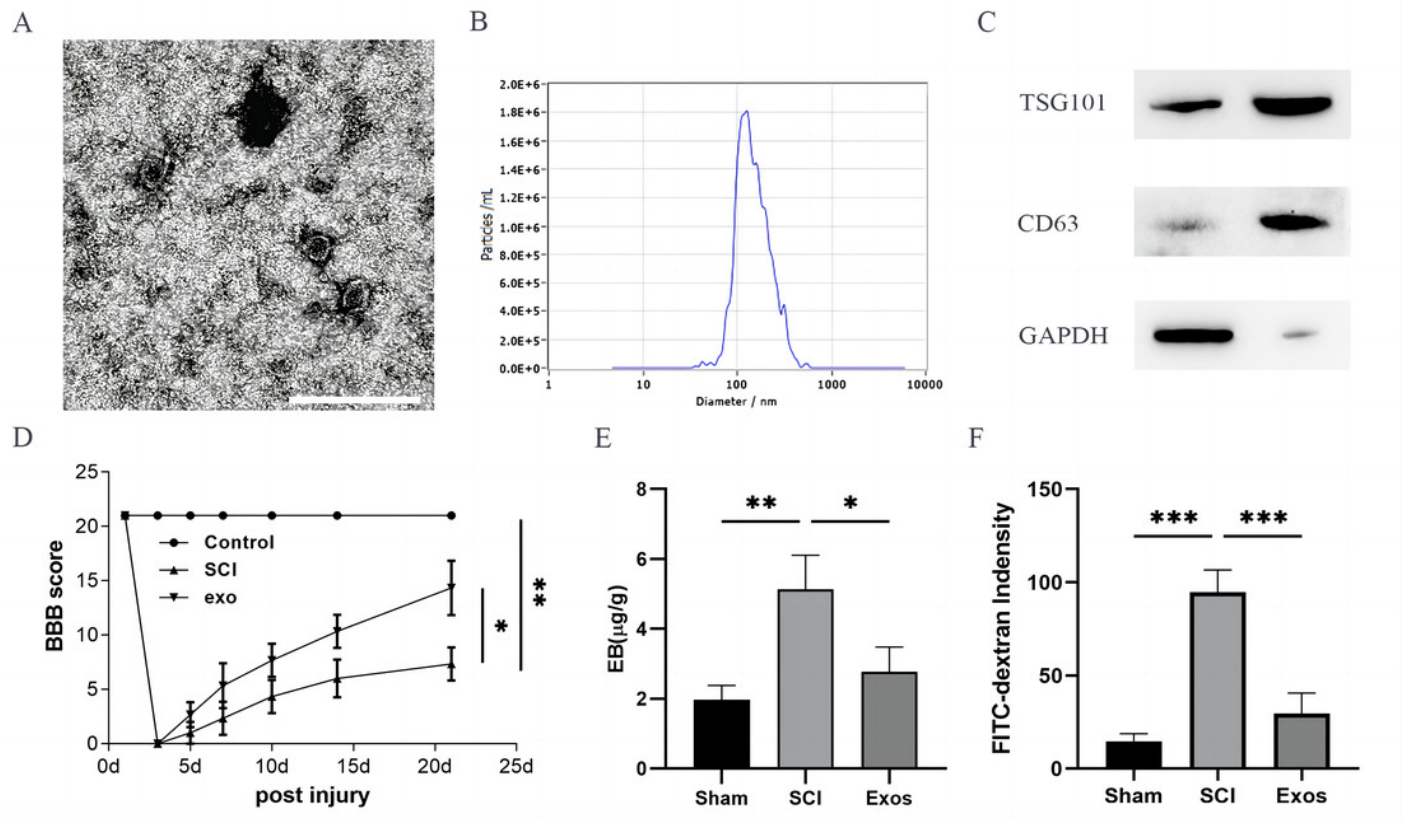

Figure 2

HUC-MSCs-Exos increase SCI-induced ET-1 production.

(A) Increased prepro-ET-1 mRNA after SCI. Expression levels of prepro-ET-1 mRNA in rat spinal cord tissue were measured at 1 days after SCI. Expression levels of prepro-ET-1 mRNA were normalized to GAPDH. Results represent mean ± SEM. *P < 0.0 5 versus the Sham group; **P < 0.01 versus sham-operated group; n = 3. (B) Increased ET-1 peptide after SCI. Production of ET-1 peptide in the spinal cord tissue was measured by ELISA at 1 days after SCI. Results represent mean ± SEM, with experimental data shown as ET-1 peptide content (ng) per spinal cord tissue weight (g). *P < 0.05 versus sham-operated group; n = 3.

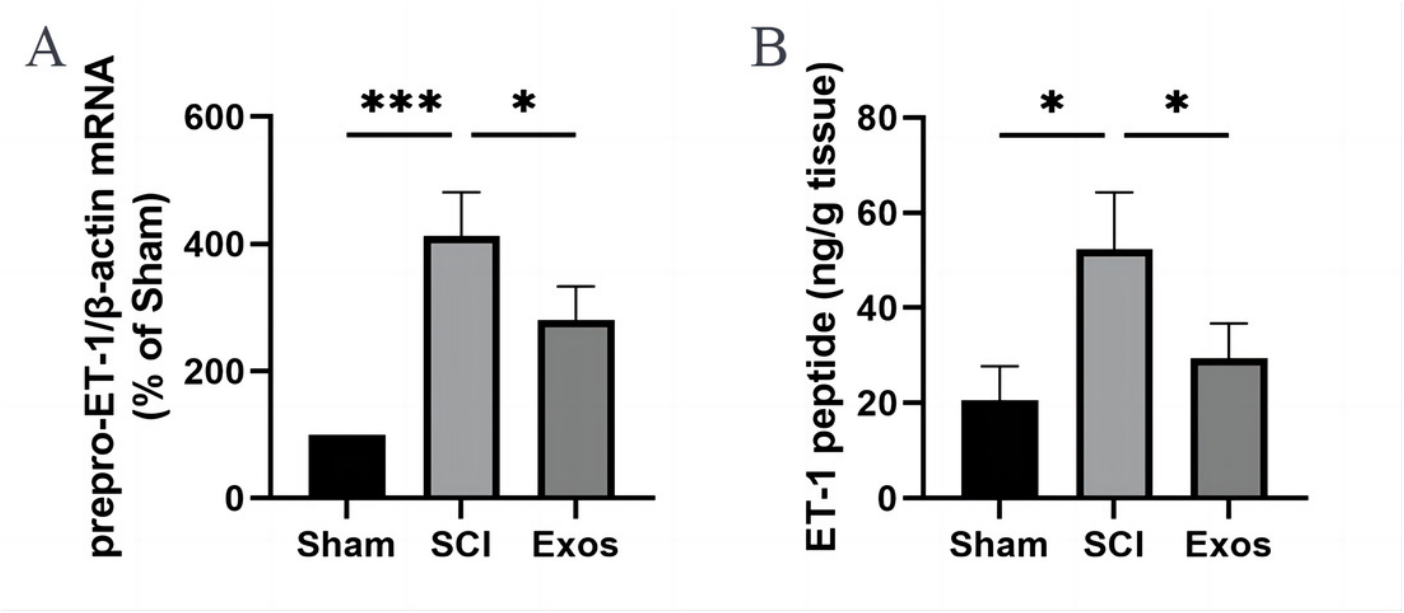

Figure 3

ET-1 is involved in the effects of hUC-MSCs-Exos on SCI repair.

(A) The BBB scores. ****P < 0.0001 versus the Sham group; n = 3. (B) Representative spinal cords show that Evans Blue dye permeabilized the injured spinal cord at 7 day; scale bar = 3mm. (C) Quantification of the amount of Evans Blue at 7day (μg/g). *P < 0.05 versus the Sham group; **P < 0.01 versus the Sham group; ***P < 0.001 versus the Sham group; n = 3. (D) FITC-dextran was used in the spinal cord peripheral penetration analysis results at 7day. ***P < 0.001 versus the Sham group; ****P < 0.0001 versus the Sham group; n = 3.

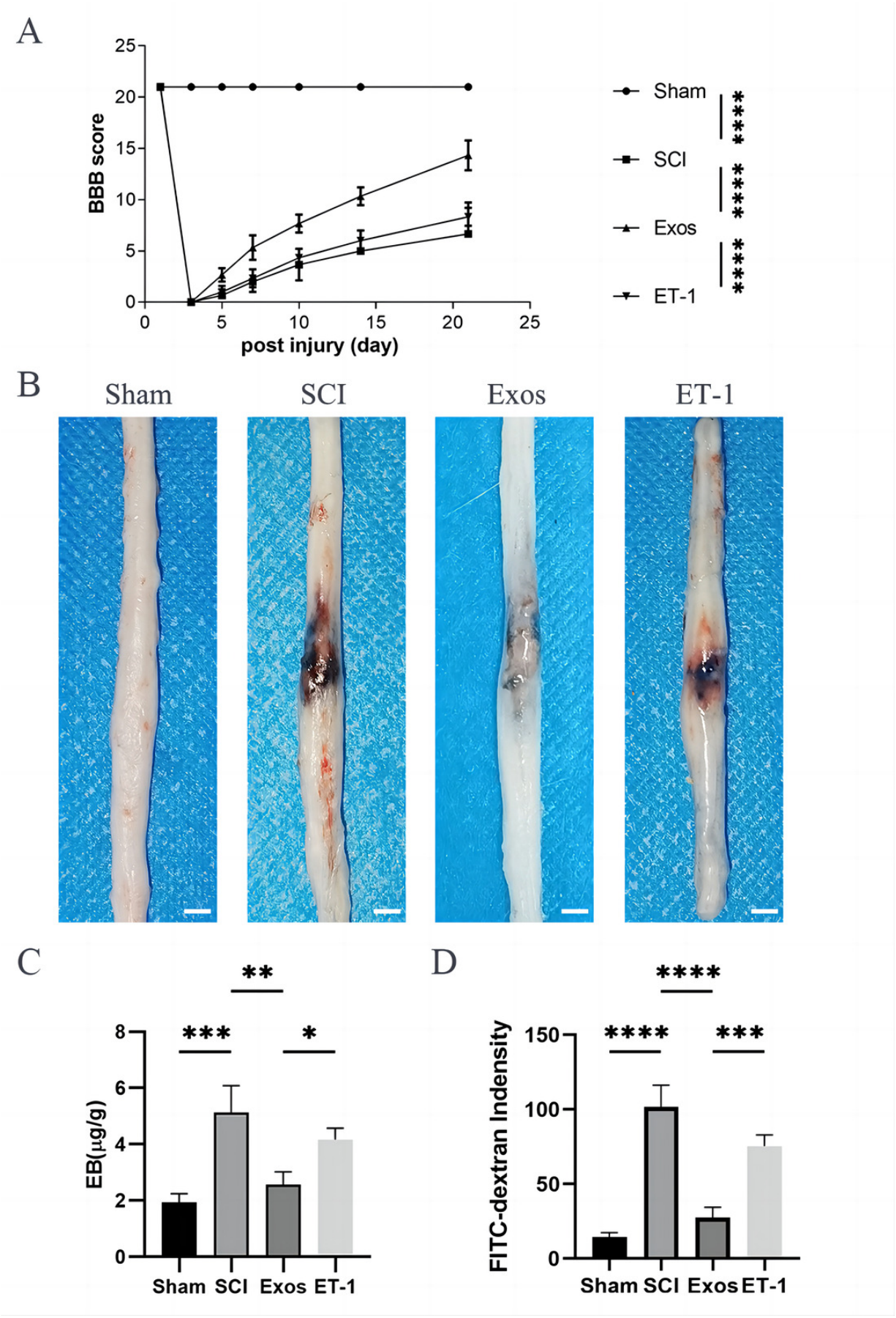
A
BBB score
post injury (day)
Sham
SCI
Exos
ET-1
B
Sham
SCI
Exos
ET-1
C
EB(μg/g)
Sham SCI Exos ET-1
D
FITC-dextran Indensity
Sham SCI Exos ET-1

Figure 4

HUC-MSCs-Exos Increase the Expression of Junction Proteins After SCI by Down-Regulation of ET-1.

(A–E) Western blot analysis of zo-1, β-catenin, occludin, and claudin-5 in the spinal cord of the sham, SCI, Exos, and ET-1 groups 1day after SCI. **P < 0.01 versus the sham group; ***P < 0.001 versus the Sham group; ****P < 0.0001 versus the Sham group; n = 3.

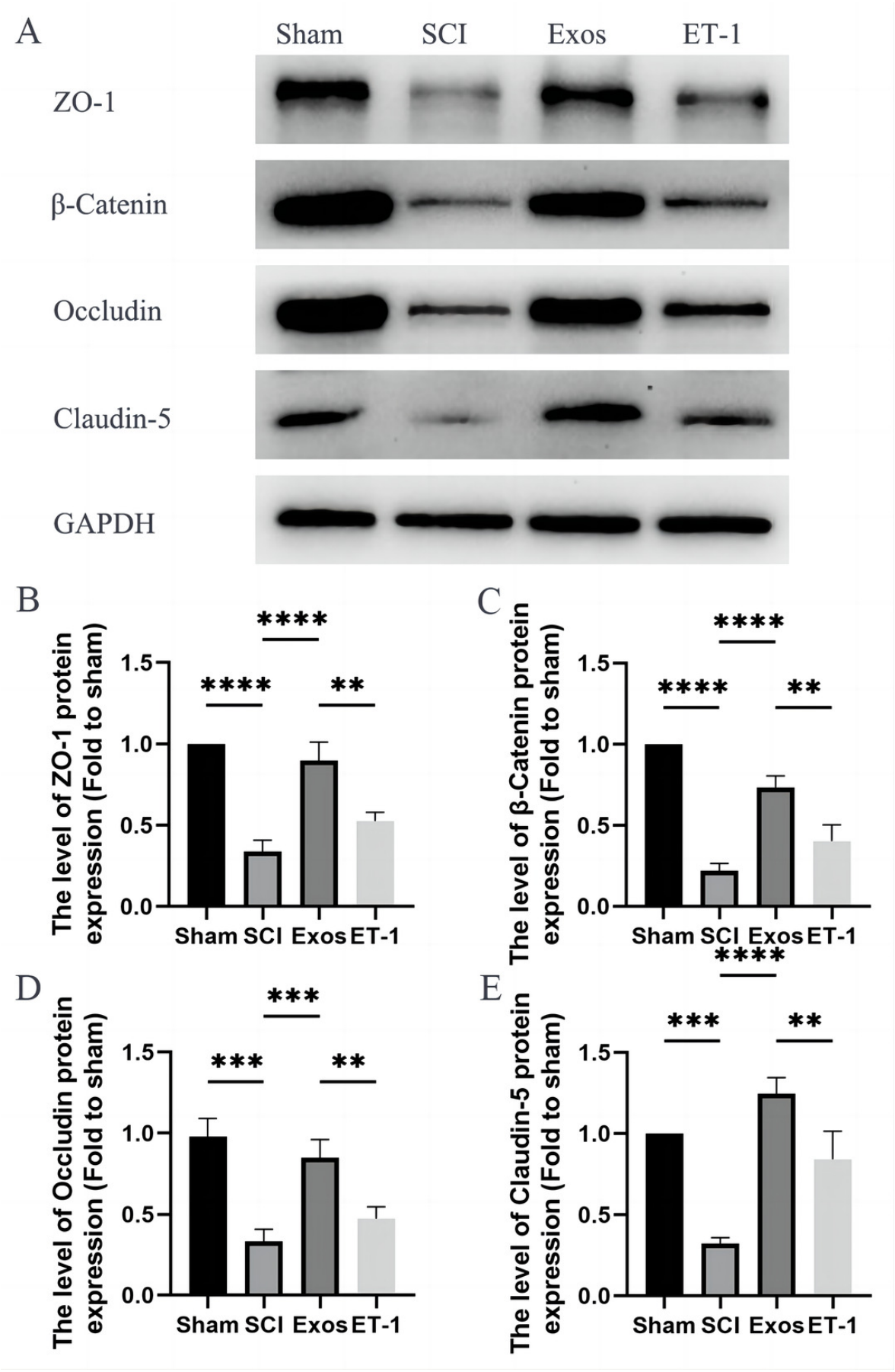
A
Sham
SCI
Exos
ET-1
ZO-1
β-Catenin
Occludin
Claudin-5
GAPDH
B
The level of ZO-1 protein expression (Fold to sham)
C
The level of β-Catenin protein expression (Fold to sham)
D
The level of Occludin protein expression (Fold to sham)
E
The level of Claudin-5 protein expression (Fold to sham)
Sham SCI Exos ET-1

Figure 5

HUC-MSCs-Exos decreases expression of inflammatory mediators in SCI rats by Down-Regulation of ET-1.

(A–C) Western blot analysis of MMP-2, and MMP-9 in the spinal cord of the sham, SCI, Exos, and ET-1 groups 1day after SCI. *P < 0.05 versus the Sham group; **P < 0.01 versus the sham group; ***P < 0.001 versus the Sham group; n = 3.

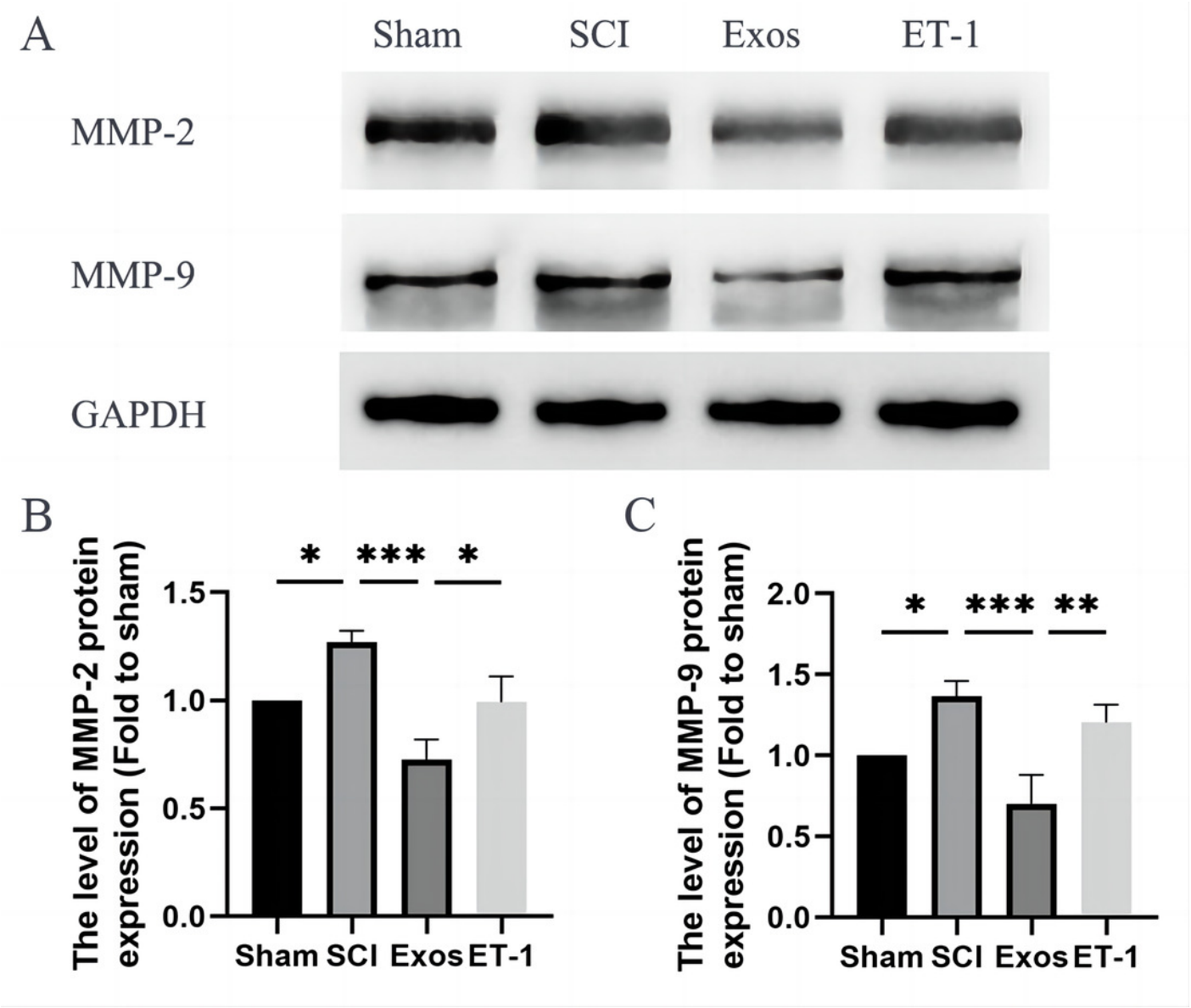

Figure 6

HUC-MSCs-Exos Increase the Expression of Junction Proteins in endothelial cells after OGD/R by Down-Regulation of ET-1.

(A–E) Western blot analysis of zo-1, β-catenin, occludin, and claudin-5 in the HBMECs of the Control, OGD/R, Exos, and ET-1 groups. *P < 0.05 versus the Control group; **P < 0.01 versus the Control group; ***P < 0.001 versus the Control group; ****P < 0.0001 versus the Control group; n = 3. (F) The viability of HBMECs of the Control, OGD/R, Exos, and ET-1 groups was tested by CCK-8 analysis. *P < 0.05 versus the Control group; ****P < 0.0001 versus the Control group; n = 3. (G) Under different conditions, FITC-dextran permeates the fluorescence intensity of the lower chamber. *P < 0.05 versus the Control group; ***P < 0.001 versus the Control group; n = 3.

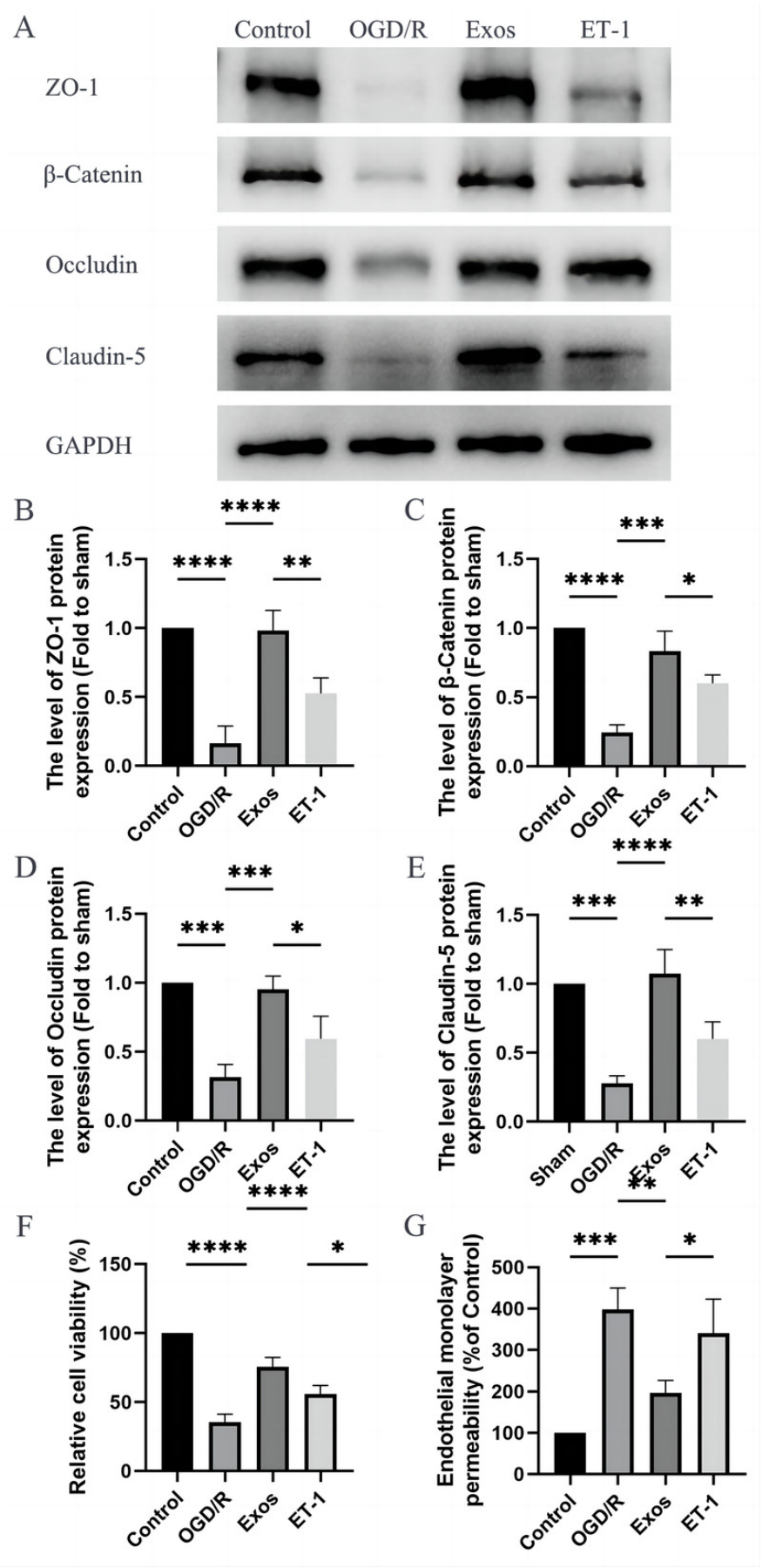
A
Control
OGD/R
Exos
ET-1
ZO-1
β-Catenin
Occludin
Claudin-5
GAPDH
B
The level of ZO-1 protein expression (Fold to sham)
C
The level of β-Catenin protein expression (Fold to sham)
D
The level of Occludin protein expression (Fold to sham)
E
The level of Claudin-5 protein expression (Fold to sham)
Sham
F
Relative cell viability (%)
G
Endothelial monolayer permeability (%of Control)